

Experimental Observation of Double-Walled Peptide Nanotubes and Monodispersity Modeling of the Number of Walls

Frédéric Gobeaux,^{†,‡} Nicolas Fay,^{†,‡} Christophe Tarabout,[‡] Florian Meneau,[§] Cristelle Mériadec,[‡] Camille Delvaux,[†] Jean-Christophe Cintrat,^{||} Céline Valéry,^{⊥,#} Franck Artzner,^{*,‡} and Maité Paternostre^{*,†}

[†]Institut de Biologie et de Technologies de Saclay/Service de Bioénergétique, Biologie Structurale et Mécanismes, UMR 8221 CNRS and CEA, CEA-Saclay, 91191 Gif-sur-Yvette, France

[‡]Institut de Physique de Rennes, UMR 6251 CNRS, Université Rennes 1, Avenue du Général Leclerc, 35042 Rennes Cedex, France

[§]SWING Beamline, SOLEIL Synchrotron, 91191 Gif-sur-Yvette, France

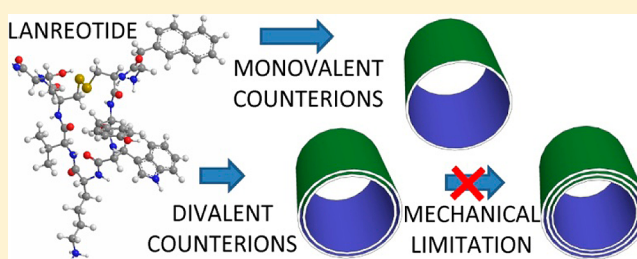
^{||}Institut de Biologie et de Technologies de Saclay/Service de Chimie Bioorganique et Marquage, CEA-Saclay, 91191, Gif-sur-Yvette, France

[⊥]Ipsen Pharma S.A., Ctra. Laurea Miro 395, 08980-Sant Feliu de Llobregat, Barcelona, Spain

[#]Biomolecular Interaction Centre, School of Biological Sciences, University of Canterbury, Christchurch, New Zealand

Supporting Information

ABSTRACT: Self-assembled nanoarchitectures based on biological molecules are attractive because of the simplicity and versatility of the building blocks. However, size control is still a challenge. This control is only possible when a given system is deeply understood. Such is the case with the lanreotide acetate, an octapeptide salt that spontaneously forms monodisperse nanotubes when dissolved into pure water. Following a structural approach, we have in the past demonstrated the possibility to tune the diameter of these nanotubes while keeping a strict monodispersity, either by chemical modification of one precise amino acid on the peptide sequence or by changing the size of the counterions. On the basis of these previous studies, we replaced monovalent counterions by divalent ones to vary the number of walls. Indeed, in the present work, we show that lanreotide associated with a divalent counterion forms double-walled nanotubes while keeping the average diameter constant. However, the strict monodispersity of the number of walls was unexpected. We propose that the divalent counterions create an adhesion force that can drive the wall packing. This adhesion force is counterbalanced by a mechanical one that is related to the stiffness of the peptide wall. By taking into account these two opposite forces, we have built a general model that fully explains why the lanreotide nanotubes formed with divalent counterions possess two walls and not more.



INTRODUCTION

Over the past decade, organic molecules of biological origin, such as lipids,¹ DNA,² or peptides,³ have been used as versatile and simple building blocks to design self-assembling nanoarchitectures such as fibers,⁴ tapes,⁵ ribbons,^{5–7} spheres,^{8,9} or tubes.^{10–14} Among these nanoarchitectures, discrete, homogeneous, and hollow cylinders with inner diameters ranging from 10 to 1000 nm will have beneficial uses in the emerging fields of bionanotechnology and related nanotechnologies.^{15–17} Indeed, such nanotubes (NTs) can be useful for designing gene carriers, submicrometer channels for capillary electrophoresis, or continuous nanoreactors for example.^{18,19}

However, in this field, the challenge still resides in gaining control over the NTs dimensions, i.e., length, diameter, and wall thickness. This control can only be achieved by a deep knowledge of the mechanism of assembly and of the nature of the interactions driving the process.

In this respect, lipids are probably the most effective building blocks for making structures at a scale ranging from nanometers

to micrometers.¹ For example, in the case of lipids that form hollow NTs, a lot of effort has been done to understand the molecular self-organization process with the aim to control the formation of nanoscale materials.²⁰ Moreover, whereas the length of a lipid NT is essentially controlled by kinetics, its radius of curvature and its wall thickness are essentially defined by the structure and the chirality of the molecule and by the packing thereof.^{1,6,7,13}

In the peptide field, the comprehension in respect of size and shape control is increasing. Aggeli et al.⁵ succeeded in predicting morphologies (i.e., twisted tapes, ribbons, or fibrils) as a function of chiral monomeric rods torsion that itself depends on concentration. They furthermore demonstrated that the twisting pitch is directly related to the thickness of the assembly. Another example comes from the lanreotide NTs.²¹

Received: December 10, 2012

Revised: January 30, 2013

Published: January 31, 2013

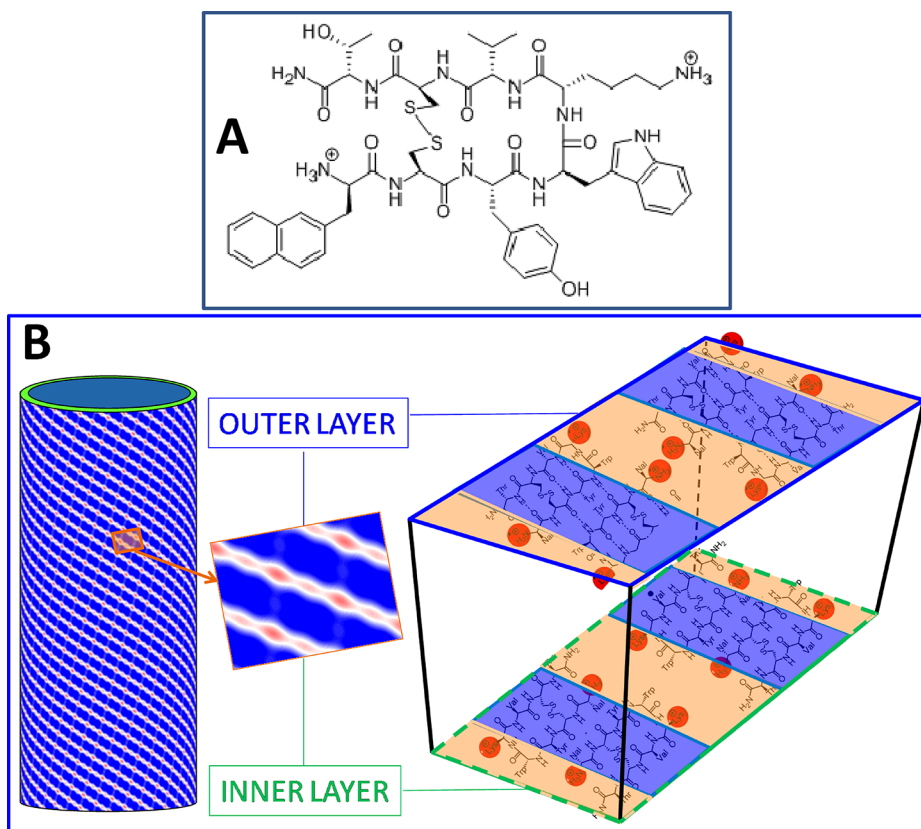


Figure 1. (A) Developed molecular structure of the lanreotide peptide. (B) From left to right: cartoon of a single-wall lanreotide nanotube with the calculated electronic density. The red areas correspond to the positively rich regions (lysine residues and N_{ter}) and the blue areas to the uncharged regions (aliphatic residues). Zoom of a small region of the nanotube wall and 2 unit cells of the lanreotide packing in the nanotube wall. Note that the two layers are different and that they have been vertically splitted for better readability. The red dots highlight the cationic charges in agreement with the nanotube cartoon.

Lanreotide is indeed a very adaptive and versatile peptide since we have already demonstrated that chemical modifications on the peptide sequence allowed generating a library of 17 peptides forming NTs of monodisperse diameters ranging from 10 to 36 nm.²² More recently, we have unveiled the structural role of the counterions in the NTs formation and that they, as a consequence, could be used to tune the NTs diameter.²³ However, although a diversity of strategies has already been put in place to gain control over length or diameter of peptide NTs in general,³ there is still a long way to reach the rationalization and control that has been achieved in the realm of lipids assembly.^{1,6,24,25} In particular, with such lipid systems, the wall thickness of NTs is controlled by molecular parameters and especially by chirality. Interestingly, in most of the cases, the multilayered lipid NTs are rather monodisperse in terms of number of layers, i.e., either 2,⁶ 3,^{12,14} 5,¹¹ or 7 layers¹² have been observed.

One of the aims of the present work is to control the wall thickness of peptide NTs using the well-studied lanreotide model system. Lanreotide is a dicationic octapeptide (sequence: H-D-2-Nal¹-cyclo(Cys²-Tyr³-D-Trp⁴-Lys⁵-Val⁶-Cys⁷)-Thr⁸-NH₂ and full structure in Figure 1A), usually manipulated as an acetate salt with a stoichiometric ratio of two acetates for one peptide. When dissolved in pure water above a critical assembly concentration (CAC) of about 15 mM, it spontaneously self-assembles into monodisperse NTs (Figure 2A).²¹ Previous studies have unraveled their structure²¹ and assembly mechanism.²⁶ In short, a lanreotide NT is built up with dimers

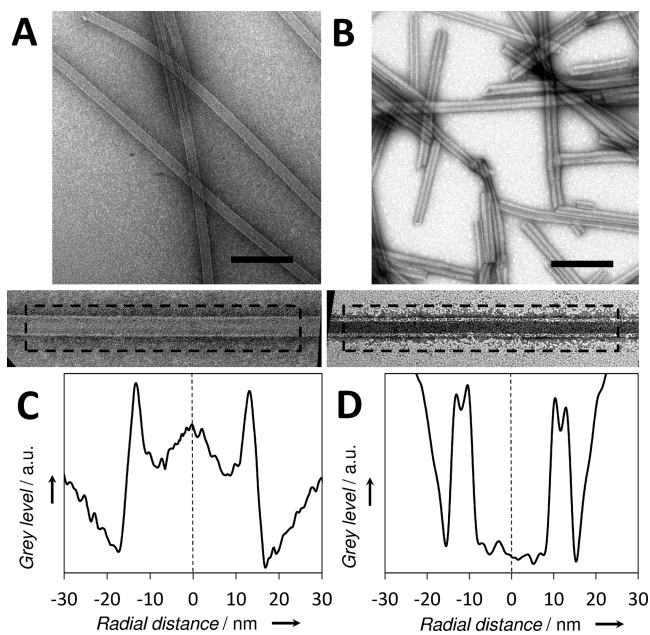


Figure 2. Negatively stained transmission electron micrographs of (A) lanreotide nanotubes with a monovalent counterion (acetate) and (B) lanreotide nanotubes with a divalent counterion (sulfate). Scale bars = 200 nm. Radial profiles of the gray level averaged along a nanotube for (C) lanreotide acetate and (D) lanreotide sulfate.

that spontaneously form in solution by segregation of aliphatic and aromatic residues. Above the CAC, the dimers self-assemble into a 2D crystal maintained by both lateral chain interactions and hydrogen bonds forming antiparallel β -sheets (Figure 1B). This crystalline peptide bilayer spontaneously bends and constitutes the NT wall, whose diameter is set by this original curvature.²⁶ Interestingly, in this system, the electrostatic is purely repulsive, counterbalancing the attractive forces such as π -stacking, H-bonds, or hydrophobic effects. The balance between repulsive electrostatics and attractive forces is the key factor that controls the monodispersity of the NTs diameter.²⁶ In particular, we have shown that 90% of the counterions are strongly adsorbed on the NTs wall and even contribute to their structure.²³

Considering the strong interaction between the self-assembled peptides and their counterions, we tested whether we could control the adhesion between different peptide bilayers and therefore govern the overall NT wall thickness by using divalent counterions. For this purpose, we replaced the acetates by dianions (with a dianion–peptide ratio of 2:1 or 1:1) such as sulfate, D-, L-, and *meso*-tartrate: the peptide is successively neutralized to remove the acetates, washed, freeze-dried, and then resolubilized in the proper amount of tartaric acid (see Materials and Methods).

We have experimentally observed the formation of double-walled NTs, thus increasing the overall NT wall thickness by a factor of 2 compared to that of single-walled lanreotide NTs formed with monovalent counterions. Moreover, we have built a model that explains that the strictly fixed number of walls possessed by such NTs results from the trade-off between the stiffness of the walls and the adhesion force between them.

MATERIALS AND METHODS

Lanreotide octapeptide was obtained from Ipsen Pharma (Barcelona, Spain) as an acetate salt powder. Acetate counterions were exchanged following the procedure exposed in refs 23 and 27: the powder—insoluble at this pH—was washed for 15 min at 4 °C with a 58 mM NaOH solution. The volume was calculated ad hoc so that the hydroxide ions neutralize all the peptide charges with only 10% excess. After several rinses with deionized water followed by centrifugation at 4 °C for 5 min at 2500g and removal of the supernatants, the pellet was freeze-dried. The dry powder containing the neutral form of the peptide could then be solubilized in an acidic solution containing enough charges of the desired counterion to reprotonate the peptide. We have displayed the results obtained with a 2:1 counterions–peptide ratio, but similar results are obtained with a 1:1 ratio (see Figure S2), although solubilization is less straightforward. After addition of deionized water to dilute the peptide solution below 1% w/w, the solution was once more freeze-dried. The obtained powder could then be dissolved in deionized water to the desired concentration.

The samples were characterized by transmission electron microscopy at 80 kV (Philips CM12, Eindhoven), Fourier transform infrared spectroscopy (Bruker IFS 66 spectrophotometer equipped with a 45° N ZnSe attenuated total reflection attachment, Karlsruhe), and small-angle X-ray scattering on the SWING beamline at SOLEIL synchrotron facility (Saint Aubin, France).

RESULTS

Above 5–10 mM in pure water, lanreotide solutions prepared with sulfate or tartrate counterions either gelify or begin to scatter light, both of which being signs of self-assembly. The morphology of the objects deposited on copper grids and negatively stained with uranyl acetate have been examined by transmission electron microscopy (TEM). Observations are still

consistent with the formation of NTs (Figure 2B). However, they seem shorter than those observed with monovalent counterions such as acetate (Figure 2A). In addition, the staining pattern is clearly different: the inside of the NTs is darker, and the clear, unstained walls appear to be slightly thicker (Figure 2C,D). After a few days of aging, bundles of these latter NTs are observed (Figure S4), which has never been the case with NTs formed in presence of monovalent counterions.

The peptide backbone conformation in the structure is assessed by attenuated total reflectance–Fourier infrared (ATR-FTIR) spectroscopy. In particular, the amide I region (1600–1800 cm^{-1}) is indicative of the inter- and intramolecular H-bonds (Figure 3A). The peak positions at 1618 and 1695

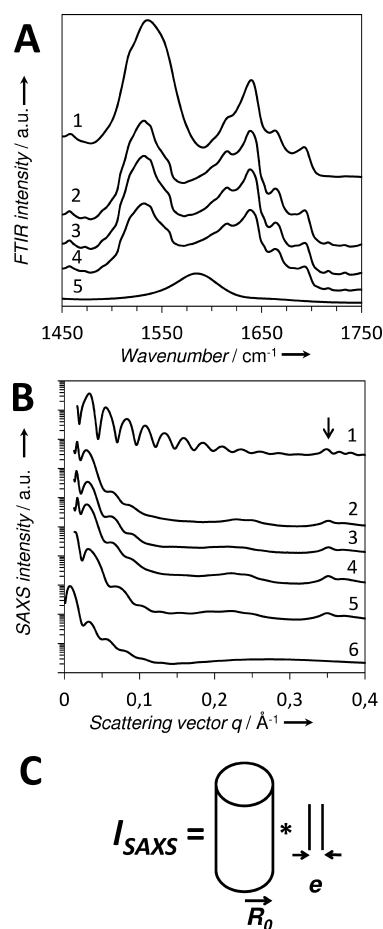


Figure 3. (A) ATR-FTIR spectra of the amide I region: 1, lanreotide acetate; 2, lanreotide-*meso*-tartrate; 3, lanreotide-D-tartrate; 4, lanreotide-L-tartrate; 5, sodium tartrate. (B) Small-angle X-ray scattering patterns of lanreotide nanotubes: 1, lanreotide acetate; 2, lanreotide-*meso*-tartrate; 3, lanreotide-D-tartrate; 4, lanreotide-L-tartrate; 5, lanreotide sulfate; 6, simulated fit for double-wall cylinders scattering. The arrow indicates the peak due to the β -sheet structure. (C) Model used for the fit of the SAXS intensity: convolution of the scattering of a cylinder and of a doubling of structure.

cm^{-1} are characteristic of antiparallel β -sheets, and the peaks positioned at 1666 and 1641 cm^{-1} are respectively attributed to a turn and a random conformation.²⁸ Such pattern is identical whether we use monovalent or divalent counterions. The original peptide packing is thus retained. The L-, *meso*-, or D-

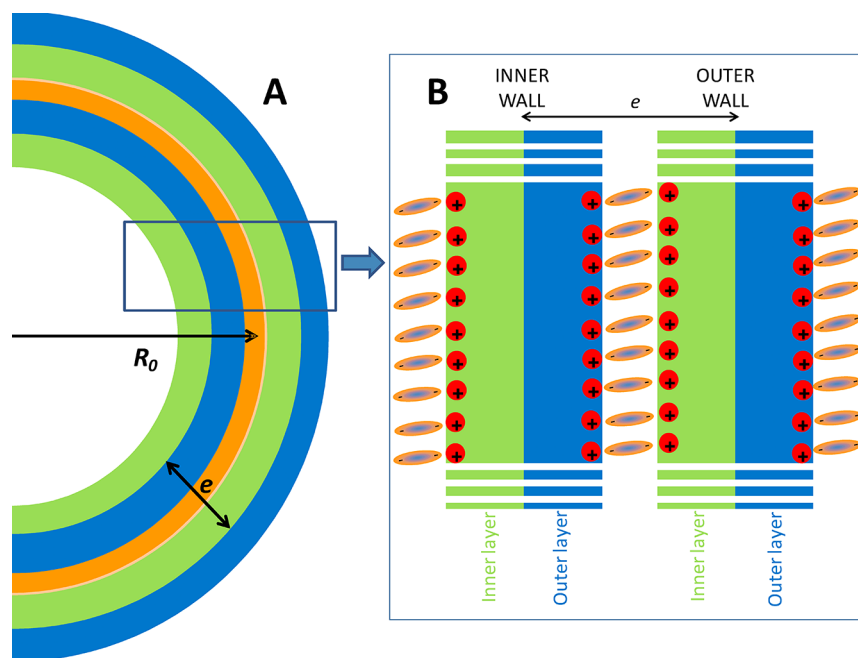


Figure 4. Sketch explaining the formation of double wall NTs. (A) Transverse section of a double wall nanotube showing the geometrical parameters R_0 and e . (B) Detail of the double-wall (longitudinal section). Each peptide wall is represented by a blue-green bilayer; the red dots represent the protonated amines (either lysine or N_{ter}) in the peptide wall. This sketch shows how the divalent counteranions could bridge two walls together. The counterions pointing toward the outside could bridge two adjacent NTs and thus may explain the bundling observed.

conformations do not to have a significant structural effect on the peptide conformation inside the walls of the NTs either.

Small-angle X-ray scattering (SAXS) experiments give further insight into the structure of the NTs (Figure 3B). In all the samples, the peak at $q = 0.35 \text{ \AA}^{-1}$ (19 \AA in direct space), corresponding to 4 times the β -sheet interstrand distance (4.7 \AA) because of the specific molecular packing of lanreotide,²⁸ corroborates the FTIR band attributions. Single-wall NTs scattering yields typical oscillations (trace 1) that can be fitted by a normalized zero-order Bessel function $J_0^2(qD_0/2)/q^2$ and provides an accurate measurement of their diameter, e.g., for lanreotide acetate NTs, $D_0 = 24.4 \text{ nm}$. In the case of the NTs formed with divalent counterions, the oscillations are fewer and a bump appears at 0.2 \AA^{-1} (traces 2–5). In fact, the intensity of the SAXS radial integration can be modeled by a zero-order Bessel function convoluted by a cosine function (trace 6) as follows:²⁹

$$I_{\text{SAXS}}(q) = I_{\text{norm}} J_0^2(qD_0/2) \cos^2(qe/2)/q^4 \quad (1)$$

where D_0 is the radius of the NTs and the convolution by a cosine function is related to the doubling of the nanostructure with a spacing e (Figure 3C). In the case of L-tartrate, for instance, we find that $D_0 = 22 \pm 1 \text{ nm}$ and $e = 2.7 \text{ nm}$, i.e., an internal diameter of $20.6 \pm 1 \text{ nm}$ and an external diameter of $23.4 \pm 1 \text{ nm}$. Moreover, the lower number of oscillations (only three to five vs more than a dozen) indicates that the double-wall NTs are more polydisperse in diameter than single-wall NTs. The fit of triple-wall NTs has also been tested and proven to be ineffective (see Figure S1). The NTs formed with divalent counterions thus possess two peptide walls.

Such double-wall NTs have been observed with both 1:1 and 2:1 counterion–peptide ratios (see Figure S2 for 1:1 ratio), which proves that a single divalent counterion can neutralize two peptide charges without impeding NT self-assembly. Moreover, when tartrate anions are made to compete with

acetate anions by adding increasing amount of sodium tartrate to a lanreotide acetate solution (Figure S3), a transition from single-wall NTs to double-wall NTs is detected as soon as the tartrate anions represent 25% of the anions in solution.

The double walls are probably linked together by sharing divalent counterions, as sketched in Figure 4B. This hypothesis is consistent with the strong adsorption of the counterions on the NT wall.²³ Moreover, zeta-potential measurements (see Table S1) indicate that the surface of the NTs is always positive, regardless of the valence of the counterions. Thus, there is no charge inversion, which eliminates the hypothesis of an attractive, electrostatically driven multilamellar formation as in the case of DNA–cationic liposomes complexes.³⁰

Although our “linker hypothesis” provides a simple explanation for the adhesion between the walls, it does not explain why the number of walls is limited to two. Indeed, since a peptide wall has two (positively) charged faces, we could have expected to pile up more walls together. This means that creating additional walls costs too much energy and that there is a competition between the energy needed to bend the walls and the energy earned thanks to the “adhesive counterions”.

To formalize the energy of the system, we propose that its free energy (E) is the sum of an adhesion energy E_{ADH} between adjacent walls and an elastic energy E_{EL} of the NT walls:

$$E = E_{\text{ADH}} + E_{\text{EL}} \quad (2)$$

For our purpose, these energies are normalized by surface unit and expressed as a function of the number of walls n . The normalized adhesion energy between adjacent walls E_{ADH} is then the product of the adhesion energy per unit area A times $(n - 1)$ interfaces between two adjacent walls divided by the total area of the interfaces (refer to the Supporting Information for calculation details):

$$E_{\text{ADH}} = -A(n - 1)/n \quad (3)$$

The normalized elastic energy E_{EL} of the NT walls is the sum of the Hooke's laws for each of the n walls divided by the total area of the NT walls (also refer to the Supporting Information):

$$E_{EL} = k(n + 1)(n - 1)e^2/12 \quad (4)$$

where k is the stiffness constant of the walls and e the spacing between the walls (see Figure 4).

In the following, we use the ratio between the surface adhesion energy and the stiffness constant, $\alpha = A/k$, as the single parameter to explore the possible configurations. Free energy plots as a function of $\sqrt{\alpha}$ are displayed in Figure 5B for

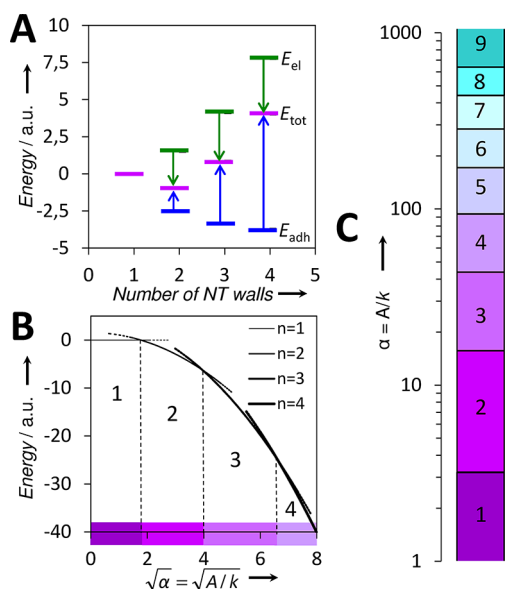


Figure 5. (A) Free energy of the multiwalled NTs for $\alpha = A/k = 5$. The free energy (magenta) is the sum of the elastic energy (green) and of the adhesion energy (blue). In these conditions, a minimum is obtained for $n = 2$ walls. (B) Simulated free energy calculated for n -walled NTs as a function of $\sqrt{\alpha}$ with $n = 1, 2, 3$, and 4. The square root is used to optimize readability of the graph. The crossings of the energy plots define the limits of the stability domains of each configuration. (C) Number of walls predicted by our model as a function of the value of the parameter $\alpha = A/k$.

different values of n . For any given α , the most stable configuration (i.e., number of walls) is the one that has the lowest free energy $E_{ADH} + E_{EL}$. The crossing of each line thus defines the limits of the domain of stability of each configuration. In the present experimental conditions, the predominance of the double-wall NTs suggests that α is in the 3.2–15.7 range. The theoretical domains of stability of the n -walled NTs as a function of α are also displayed in Figure 5C. All these domains are very wide, and each n -walled configuration is very stable and not sensitive to small fluctuations. The only parameters that could be used to change the number of walls are A , k , and e . Experimentally, the latter two are intrinsic to the system, and although it could be envisioned to modify the adhesion energy by using another type of counterion, we cannot expect to change it over several orders of magnitude. Indeed, to increase the number of walls from n to $n + 1$, one must add an adhesion energy varying as

$$A = -kn(n + 1)(2n + 1)e^2/12 \quad (5)$$

This model thus suggests that the number of walls is controlled by the free energy of the system. Indeed, since this energy is the

sum of a positive elastic contribution (destabilizing component) and a negative adhesion energy (stabilizing component), there is a minimum that sets the number of walls (see Figure 5A). This model can be likened to the one used to describe the self-assembly of chiral rodlike units, in which the elastic energy originates from the torsion inside fibrils.⁵

Finally, this well-defined tuning of the number of walls explains why we rather observe bundles of double-walled NTs instead of multiwalled NTs. Indeed, the adhesion between adjacent NTs is certainly permitted by the same process of sharing divalent counterions. Incidentally, if the peptide concentration is increased up to 30% w/w, a higher number of walls (“embedded NTs”) can be obtained with monovalent counterions.²⁸ In this case, the attraction between walls is probably enhanced by the volume reduction as are the helical tapes observed by Aggeli et al.⁵

Since we measured that the average radius R_0 of a double-walled NT is 1–2 nm smaller than the radius of the lanreotide acetate NTs, we also calculated in the framework of the present model a contraction term Δ defined as the difference between the average radius of a n -wall NT and the radius of an equivalent single-wall NT (see details in Supporting Information). This term was found to be -0.2 nm, a value negligible compared to the specific counterion effect that we have previously reported.²³ The measured lowering of the NT average diameter is thus most likely due to a lesser steric hindrance of the counterion than to elastic contraction.

In conclusion, we have presented in this report a new way to modulate the interaction between the walls of peptide NTs. We showed that we could form double-wall peptide NTs by simply replacing the monovalent counterions—or only a fraction thereof—by divalent ones. The morphological control in other multilayered supramolecular systems rather relies on modification of molecular structure,¹³ chirality,^{7,12} concentration,^{5,13} or solvent conditions.^{31,32} We have also proposed a model explaining that the competition between the adhesion energy and the curvature limits the number of NT walls to two. A comparable model had been proposed by Aggeli et al. to explain the limited width of twisted fibrils.⁵ Ours could be used to describe other nanotubular systems such as metallosilicate multiwalled NTs for which the origin of the adhesion is of a very different nature (i.e., attraction of oppositely charged walls) but whose wall number seems similarly limited.³³ In the end, combining these results to those of previous studies on lanreotide,²² we have in our hands a nanotubular peptide system whose both diameter and number of walls can be controlled, which is a unique feature in the self-assembling peptide domain. This unprecedented mastery could pave the way toward adaptable and versatile applications.

■ ASSOCIATED CONTENT

Supporting Information

Table of zeta-potential measurements, different fits for the SAXS profiles, full characterization of 1:1 lanreotide tartrate sample, SAXS profiles of acetate/tartrate competition experiments, and detailed calculation for the model of multiwalled NTs free energy. This material is available free of charge via the Internet at <http://pubs.acs.org>.

■ AUTHOR INFORMATION

Corresponding Author

*E-mail franck.artzner@univ-rennes1.fr, fax +33 2 23 23 56 45 (F.A.); e-mail maite.paternostre@cea.fr, fax +33 1 69 08 67 49 (M.P.).

Notes

The authors declare no competing financial interest.

■ ACKNOWLEDGMENTS

This work was supported by the biotechnology program of the French Agency for Research (ANR) with the SmartPep project. F.G. and N.F. were funded by Commissariat à l'Énergie Atomique et aux Énergies Alternatives. C.T. was funded by the Région Bretagne through a Ph.D. fellowship. Synchrotron SOLEIL (France) is acknowledged for beam time allocation. The TEM-team platform (iBiTec-S/SB2SM) is also acknowledged.

■ REFERENCES

- (1) Shimizu, T.; Masuda, M.; Minamikawa, H. Supramolecular nanotube architectures based on amphiphilic molecules. *Chem. Rev.* **2005**, *105* (4), 1401–1443.
- (2) Pinheiro, A. V.; Han, D. R.; Shih, W. M.; Yan, H. Challenges and opportunities for structural DNA nanotechnology. *Nat. Nanotechnol.* **2011**, *6* (12), 763–772.
- (3) Valery, C.; Artzner, F.; Paternostre, M. Peptide Nanotubes: molecular organisations, self-assembly mechanisms and applications. *Soft Matter* **2011**, *7*, 9583–9594.
- (4) Hamley, I. W. Peptide fibrillation. *Angew. Chem., Int. Ed.* **2007**, *46* (43), 8128–8147.
- (5) Aggeli, A.; Nyrkova, I. A.; Bell, M.; Harding, R.; Carrick, L.; McLeish, T. C. B.; Semenov, A. N.; Boden, N. Hierarchical self-assembly of chiral rod-like molecules as a model for peptide beta-sheet tapes, ribbons, fibrils, and fibers. *Proc. Natl. Acad. Sci. U. S. A.* **2001**, *98* (21), 11857–11862.
- (6) Oda, R.; Artzner, F.; Laguerre, M.; Huc, I. Molecular structure of self-assembled chiral nanoribbons and nanotubules revealed in the hydrated state. *J. Am. Chem. Soc.* **2008**, *130* (44), 14705–14712.
- (7) Oda, R.; Huc, I.; Schmutz, M.; Candau, S. J.; MacKintosh, F. C. Tuning bilayer twist using chiral counterions. *Nature* **1999**, *399* (6736), 566–569.
- (8) Adler-Abramovich, L.; Gazit, E. Controlled patterning of peptide nanotubes and nanospheres using inkjet printing technology. *J. Pept. Sci.* **2008**, *14* (2), 217–223.
- (9) Adler-Abramovich, L.; Kol, N.; Yanai, I.; Barlam, D.; Shneck, R. Z.; Gazit, E.; Rousso, I. Self-assembled organic nanostructures with metallic-like stiffness. *Angew. Chem., Int. Ed.* **2010**, *49* (51), 9939–9942.
- (10) Hartgerink, J. D.; Granja, J. R.; Milligan, R. A.; Ghadiri, M. R. Self-assembling peptide nanotubes. *J. Am. Chem. Soc.* **1996**, *118* (1), 43–50.
- (11) Yui, H.; Minamikawa, H.; Danev, R.; Nagayama, K.; Kamiya, S.; Shimizu, T. Growth process and molecular packing of a self-assembled lipid nanotube: Phase-contrast transmission electron microscopy and XRD analyses. *Langmuir* **2008**, *24* (3), 709–713.
- (12) Thomas, B. N.; Lindemann, C. M.; Corcoran, R. C.; Cotant, C. L.; Kirsch, J. E.; Persichini, P. J. Phosphonate lipid tubules II. *J. Am. Chem. Soc.* **2002**, *124* (7), 1227–1233.
- (13) Spector, M. S.; Selinger, J. V.; Singh, A.; Rodriguez, J. M.; Price, R. R.; Schnur, J. M. Controlling the morphology of chiral lipid tubules. *Langmuir* **1998**, *14* (13), 3493–3500.
- (14) Imae, T.; Funayama, K.; Krafft, M. P.; Giulieri, F.; Tada, T.; Matsumoto, T. Small-angle scattering and electron microscopy investigation of nanotubules made from a perfluoroalkylated glucophospholipid. *J. Colloid Interface Sci.* **1999**, *212* (2), 330–337.
- (15) de la Rica, R.; Matsui, H. Applications of peptide and protein-based materials in bionanotechnology. *Chem. Soc. Rev.* **2010**, *39* (9), 3499–3509.
- (16) Lakshmanan, A.; Zhang, S. G.; Hauser, C. A. E. Short self-assembling peptides as building blocks for modern nanodevices. *Trends Biotechnol.* **2012**, *30* (3), 155–165.
- (17) Petrov, A.; Audette, G. F. Peptide and protein-based nanotubes for nanobiotechnology. *Wiley Interdiscip. Rev.: Nanomed. Nanobiotechnol.* **2012**, *4* (5), 575–585.
- (18) Liang, N. N.; Zhang, B. Impact of nanomaterials on high throughput separation methodologies. *Comb. Chem. High Throughput Screening* **2011**, *14* (3), 182–190.
- (19) Pradeep, H.; Rajanikant, G. K. Nanochannels: biological channel analogues. *IET Nanobiotechnol.* **2012**, *6* (2), 63–70.
- (20) Singh, A.; Wong, E. M.; Schnur, J. M. Toward the rational control of nanoscale structures using chiral self-assembly: Diacetylenic phosphocholines. *Langmuir* **2003**, *19* (5), 1888–1898.
- (21) Valery, C.; Paternostre, M.; Robert, B.; Gulik-Krzywicki, T.; Narayanan, T.; Dedieu, J. C.; Keller, G.; Torres, M. L.; Cherif-Cheikh, R.; Calvo, P.; Artzner, F. Biomimetic organization: Octapeptide self-assembly into nanotubes of viral capsid-like dimension. *Proc. Natl. Acad. Sci. U. S. A.* **2003**, *100* (18), 10258–10262.
- (22) Tarabout, C.; Roux, S.; Gobeaux, F.; Fay, N.; Pouget, E.; Meriadec, C.; Ligeti, M.; IJsselstijn, M.; Besselievre, F.; Buisson, D.; Verbavatz, J.-M.; Petitjean, M.; Valéry, C.; Perrin, L.; Rousseau, B.; Artzner, F.; Paternostre, M.; Cintrat, J.-C. Control of peptide nanotube diameter by chemical modifications of an aromatic residue involved in a single close contact. *Proc. Natl. Acad. Sci. U. S. A.* **2011**, *108* (19), 7679–7684.
- (23) Gobeaux, F.; Fay, N.; Tarabout, C.; Mériadec, C.; Meneau, F.; Ligeti, M.; Buisson, D.-A.; Cintrat, J.-C.; Nguyen, K. M. H.; Perrin, L.; Valéry, C.; Artzner, F.; Paternostre, M. Structural role of counterions adsorbed on self-assembled peptide nanotubes. *J. Am. Chem. Soc.* **2012**, *134*, 723–733.
- (24) Masuda, M.; Shimizu, T. Multilayer structure of an unsymmetrical monolayer lipid membrane with a 'head-to-tail' interface. *Chem. Commun.* **2001**, *23*, 2442–2443.
- (25) Masuda, M.; Shimizu, T. Lipid nanotubes and microtubes: Experimental evidence for unsymmetrical monolayer membrane formation from unsymmetrical bolaamphiphiles. *Langmuir* **2004**, *20* (14), 5969–5977.
- (26) Pouget, E.; Fay, N.; Dujardin, E.; Jamin, N.; Berthault, P.; Perrin, L.; Pandit, A.; Rose, T.; Valery, C.; Thomas, D.; Paternostre, M.; Artzner, F. Elucidation of the self-assembly pathway of lanreotide octapeptide into beta-sheet nanotubes: Role of two stable intermediates. *J. Am. Chem. Soc.* **2010**, *132* (12), 4230–4241.
- (27) Roux, S.; Zekri, E.; Rousseau, B.; Paternostre, M.; Cintrat, J. C.; Fay, N. Elimination and exchange of trifluoroacetate counter-ion from cationic peptides: a critical evaluation of different approaches. *J. Pept. Sci.* **2008**, *14* (3), 354–359.
- (28) Valery, C.; Artzner, F.; Robert, B.; Gulick, T.; Keller, G.; Grabielle-Madellmont, C.; Torres, M. L.; Cherif-Cheikh, R.; Paternostre, M. Self-association process of a peptide in solution: From beta-sheet filaments to large embedded nanotubes. *Biophys. J.* **2004**, *86* (4), 2484–2501.
- (29) Pouget, E.; Dujardin, E.; Cavalier, A.; Moreac, A.; Valery, C.; Marchi-Artzner, V.; Weiss, T.; Renault, A.; Paternostre, M.; Artzner, F. Hierarchical architectures by synergy between dynamical template self-assembly and biomineralization. *Nat. Mater.* **2007**, *6* (6), 434–439.
- (30) Rädler, J. O.; Koltover, I.; Salditt, T.; Safinya, C. R. Structure of DNA-cationic liposome complexes: DNA intercalation in multilamellar membranes in distinct interhelical packing regimes. *Science* **1997**, *275* (5301), 810–814.
- (31) Ratna, B. R.; Baraltosh, S.; Kahn, B.; Schnur, J. M.; Rudolph, A. S. Effect of alcohol chain-length on tubule formation in 1,2-bis(10,12-tricosadiynoyl)-sn-glycero-3-phosphocholine. *Chem. Phys. Lipids* **1992**, *63* (1–2), 47–53.

(32) Spector, M. S.; Selinger, J. V.; Schnur, J. M. Thermodynamics of phospholipid tubules in alcohol/water solutions. *J. Am. Chem. Soc.* **1997**, *119* (36), 8533–8539.

(33) (a) Thill, A.; Maillet, P.; Guiose, B.; Spalla, O.; Belloni, L.; Chaurand, P.; Auffan, M.; Olivi, L.; Rose, J. Physico-chemical control over the single or double wall structure of aluminogermanate imogolite-like nanotubes. *J. Am. Chem. Soc.* **2012**, *134*, 3780–3786.

(b) Thill, A.; Guiose, B.; Bacia-Verloop, M.; Geertsen, V.; Belloni, L. How the diameter and structure of $(\text{OH})_3\text{Al}_2\text{O}_3\text{Si}_x\text{Ge}_{1-x}\text{OH}$ imogolite nanotubes are controlled by an adhesion versus curvature competition. *J. Phys. Chem. C* **2013**, *116* (51), 26841–26849.